The Investigation of Compositional, Structural and Dynamical Changes of PTZ-induced Seizures on a Rat Brain by FTIR Spectroscopy.

ARTICLE *in* ANALYTICAL CHEMISTRY · DECEMBER 2013

Impact Factor: 5.64 · DOI: 10.1021/ac402992j · Source: PubMed

4 AUTHORS, INCLUDING:

Mete Severcan
Middle East Technical University
32 PUBLICATIONS **242** CITATIONS

SEE PROFILE

Feride Severcan
Middle East Technical University
162 PUBLICATIONS **2,004** CITATIONS

SEE PROFILE

analytical chemistry

Article

pubs.acs.org/ac

Investigation of Compositional, Structural, and Dynamical Changes of Pentylenetetrazol-Induced Seizures on a Rat Brain by FT-IR Spectroscopy

Sevgi Turker,[†,‡] Gul Ilbay,[§] Mete Severcan,[∥] and Feride Severcan[‡,*]

[‡]Department of Biological Sciences, Middle East Technical University, Ankara, 06531, Turkey

[†]Department of Biology, Kocaeli University, Kocaeli, 41900, Turkey

[§]Department of Physiology, Faculty of Medicine, Kocaeli University, Kocaeli, 41900, Turkey

[∥]Department of Electrical and Electronic Engineering, Middle East Technical University, Ankara, 06531, Turkey

Supporting Information

ABSTRACT: To accomplish the appropriate treatment strategies of epilepsy action mechanisms underlying epileptic seizures should be lightened. The identification of epileptic seizure-induced alterations on the brain related to their pathologies may provide information for its action mechanism. Therefore, the current study determined molecular consequences of seizures induced by pentylenetetrazol (PTZ), which is a widely used convulsant agent, on rat brain. The rats were administered subconvulsant (25 mg/kg) and convulsant (60 mg/kg) doses of PTZ during a week, and brain tissues were studied by Fourier transform infrared (FT-IR) spectroscopy. Results revealed a decrease in lipid fluidity and lipid and protein content and also the differences in membrane packing by changing the nature of hydrogen bonding as indicated by the C═O, the PO^-_2 symmetric, and asymmetric bands. Monitoring of the olefinic band elicited seizure-induced lipid peroxidation further confirmed by the thiobarbituric acid (TBAR) assay. Additionally, PTZ-induced convulsions led to alterations in protein structures obtained by neural network (NN) predictions like an increase in random coils. On the basis of the spectral changes, treated samples could be successfully differentiated from the controls by cluster analysis. Consequently, the convulsive dose of PTZ caused more significant molecular variations compared to the subconvulsive one. All findings might have an important role in understanding the molecular mechanisms underlying epileptic activities.

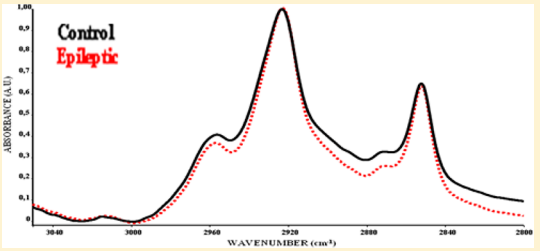

Epilepsies are a heterogeneous group of symptom complexes whose common feature is the recurrence of seizures. An epileptic seizure originating from the activation of a group of neurons at the same time is a sudden onset of symptoms and clinical manifestations caused by an abnormal, excessive, hypersynchronous burst of electrical activity that disrupts brain functions.[1,2] Patients who develop epilepsy demonstrate progression in both number of seizures and in seizure-related neurological symptoms such as cognitive and behavioral disorders. Although it is a well-known disorder, epileptic seizures can remain uncontrollable in at least 30% of all the cases.[2,3]

As widely used epileptic models, pentylenetetrazol (PTZ)-induced models show basic physiological and behavioral changes that are directly associated with the pathological consequences found in humans.[4] This epileptogenic agent has been shown to interact with the extracellular domain of the chloride channel complex[5] and neurotransmitter receptors.[6] Moreover, PTZ has the ability to affect the GABAa receptor[7] and potassium channel intracellularly.[8] However, it is worth mentioning that its action mechanism is restricted by composition and species of membrane lipids as recently shown in our study.[9]

Once developed, an epileptic condition may not be viewed as a random succession of seizures, but the dynamic process still results in functional and structural abnormalities in the brain. There are limited number of studies mostly at the clinical level reporting these biochemical and functional alterations by single and repeated administration of PTZ.[10,11] All attempt to understand the progression of epilepsy,[12] but a better understanding of molecular mechanisms of epileptic activities is required to promote new advances in the development of antiepileptic drugs resulting in a complete cure. Therefore, the determination of molecular changes induced by epileptic seizures correlated with their pathology can provide novel insight to understand the action mechanisms of epileptic activities.[13] These alterations could be successfully monitored by Fourier transform infrared (FT-IR) spectroscopy as in previous studies performed on different pathological conditions.[14−17] This technique is nondisturbing and shows high sensitivity in simultaneously detecting the changes in the functional groups belonging to tissue components.[17−24] The

Received: January 7, 2013
Accepted: December 30, 2013
Published: December 30, 2013

shifts in peak positions, bandwidth, and peak area/intensity values give valuable information which can be used for rapid and proper identification of disease states in a variety of biological samples such as tissues, membranes, cells, and biofluids. Thus, in recent years, this method has been commonly used for diagnosis of several diseases.[18−24] In the present study, we aimed to investigate compositional, structural, and functional changes resulting from PTZ-induced convulsions on rat brain homogenates by FT-IR spectroscopy, which to the best of our knowledge has not been reported previously.

EXPERIMENTAL SECTION

Chemicals. Penthylenetetrazol (PTZ), sucrose, trizma base, ethylene diamine tetra acetic acid (EDTA), phenylmethylsulfonylfluoride (PMSF), buthylatedhyroxytoluene, and thiobarbituric acid were purchased from Sigma (Sigma Chemical Co., St. Louis, MO, USA). Trichloroacetic acid and hydrochloric acid were purchased from Merck. All chemicals were used without further purification.

Animals. All procedures were conducted in accordance with welfare guidelines approved by the Ethics Committee (KOU-44543) and carried out on male Wistar rats weighing 200−250 g. Animals were allowed free access to rat food and tap water and were housed in a room under a constant 12 h light/dark cycle with humidity of 10−50%. The animals were divided into three different groups as control (n = 7), subconvulsant (n = 6), and convulsant (n = 7). During a week, while the control group was administered physiological saline, subconvulsant and convulsant groups received 25 and 60 mg/kg doses of PTZ, respectively. Both PTZ groups were placed in glass cages to record the seizure intensities after injections. In the subconvulsant group, i.p. tonic-clonic seizures were not observed. The seizure intensities were evaluated on the basis of Racine's scale[25] (Supporting Information, Table 1). Later, the animals were sacrificed by decapitation, and the brains were quickly dissected.

Sample Preparation for FT-IR Study. For the sample preparation of the FT-IR study, the same approach was used as performed in our other studies and in the other reports in the literature.[23,24,26,27] Whole brain samples were weighed, resuspended, and chopped in buffer (0.25 M sucrose, 10 mM Tris−HCl, pH 7.4, 1 mM EDTA, and 1 mmol PMSF) using a volume that is 5 times the weight of the sample. The samples were homogenized using a Potter Elvehem type glass-Teflon homogenizer and centrifuged at 100 000g for 1 h at 4 °C. The pellet fraction containing all structural parts of the tissue was acquired. The aliquots were stored at −70 °C until they were used.

FT-IR Spectroscopic Study and Data Analysis. FT-IR spectra were recorded at 4000−600 cm^{-1}. Fifteen μL samples were placed between ZnSe windows with a Teflon spacer to give 12 μm sample thickness. IR spectra were obtained using a Perkin-Elmer spectrometer equipped with a deuterated triglycine sulfate (DTGS) detector. In order to get rid of the atmospheric water vapor and carbon dioxide interference background spectra collected under identical conditions were automatically subtracted from the sample spectra. Interferograms were averaged for 200 scans at 2 cm^{-1} resolution. To check the accuracy of the absorbance values, to minimize intrasample variability, and to eliminate any possible variation that might arise from experimental conditions, three independent aliquots from the same homogenate belonging to each animal were recorded. All gave identical spectra as illustrated in Figure S-1 in the Supporting Information. Using the Perkin-Elmer Spectrum One software program, these three replicates were averaged to represent the spectrum of one animal. This procedure was repeated for all animals. The average spectra were then used for data evaluation and statistical analysis.

Since the water content interferes with IR spectra by overlapping the bands of proteins (1700−1500 cm^{-1}) and lipids (3050−2800 cm^{-1}), the buffer spectrum was subtracted from the sample spectra. To remove water absorption bands and to eliminate any interference of the chemicals in buffer, the spectra of homogenization buffer were subtracted from each sample spectrum using the same software program. In the subtraction process, the water band located around 2125 cm^{-1} was flattened (Supporting Information, Figure S-2).

For the determination of the variations in the peak areas, peak positions, and bandwidths, each original spectrum was analyzed using the Spectrum One software program. The calculations of peak area ratios were given in detail in the Supporting Information. The band positions were measured as the center of the weight (the center of 80% height of the peak). The bandwidth values were calculated as the width at 0.80 × height of the signal in terms of cm^{-1}.

The software was also used for baseline correction, normalization, and deconvolution. Besides that the water subtraction process gives residual baseline to all spectra, we further applied additional linear baseline correction to all sample spectra with the respect to 4000, 2750, 1800, and 1000 cm^{-1} base points. Additionally, we performed deconvolution only in the C−H region covering 3050−2800 cm^{-1} with 0.7 gamma factor. The baseline correction, normalization, and deconvolution processes were applied only for visual representation of the differences. For the accurate determination of the mean values for the band areas, the band positions, and the bandwidth values, the original average spectrum (from three replicates) belonging to each individual of the groups was taken into consideration.

Protein Secondary Structure Determination by Neural Network. For the determination of the variations in protein secondary structure, the amide I band between 1700 and 1600 cm^{-1}h was utilized. The neural networks (NNs) were first trained using FT-IR spectra of 18 water-soluble proteins whose secondary structures are known from X-ray crystallographic analysis.[28] Since the training data set was small in size, to improve the generalization ability of the trained NNs, and to improve the prediction accuracy, the following preprocessing steps were applied during training: Data vectors formed from the sample values of the spectra over the amide I band were first amplitude normalized; then, the number of training vectors were quadrupled by interpolation while in the same manner interpolating the target values, i.e., secondary structure values obtained from X-ray crystallography; finally, discrete cosine transform of the resulting vectors was obtained to train the NNs. The Bayesian regularization method was applied to train the NNs. For each structure, a separate NN was modeled with an optimum number of inputs and hidden neurons. During the prediction step, the same preprocessing steps were applied to the sample spectra which were obtained under the same conditions as the reference spectra used for training. The processed vectors were applied to the optimized NNs obtained from the training step to get predictions. The details of the training and testing algorithm can be found in Severcan et al.[29]

dx.doi.org/10.1021/ac402992j | Anal. Chem. 2014, 86, 1395−1403

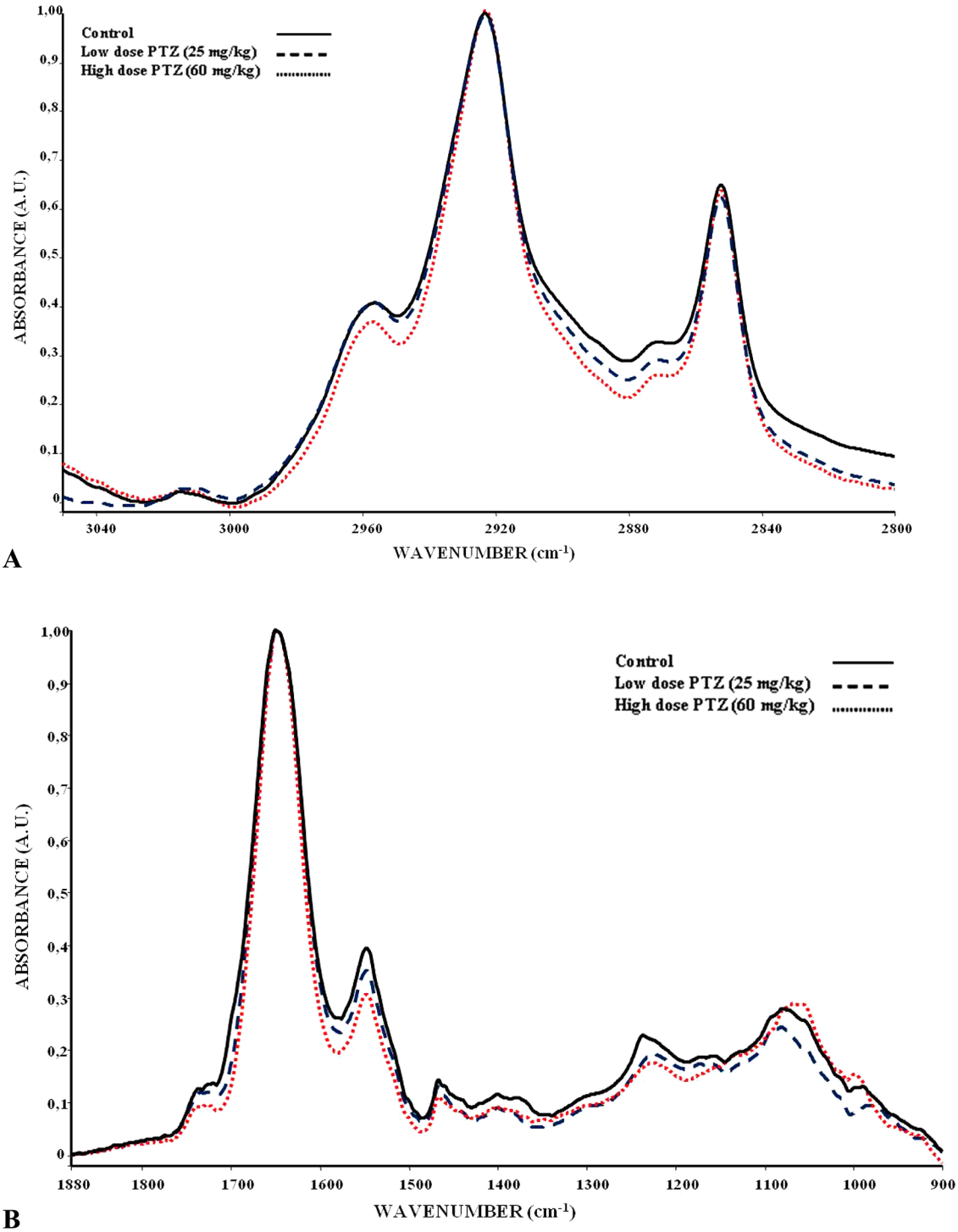

Figure 1. (A) Representative FT-IR spectra of control, low dose, and high dose of PTZ in the region of 3050−2800 cm^{-1}. (The spectra were normalized with respect to the CH_2 asymmetric stretching at 2925 cm^{-1}.) (B) Representative FT-IR spectra of control, low dose, and high dose of PTZ in the region of 2000−900 cm^{-1}. (The spectra were normalized with respect to the amide I at 1645 cm^{-1}.)

Measurement of Lipid Peroxidation (Thiobarbituric Acid (TBAR) Assay). TBARS, a well-adopted test, was performed to monitor lipid peroxidation end products[18] as briefly given in the Supporting Information.

Cluster Analysis. Hierarchical cluster analysis was performed on the spectra using the thirteen smoothing point Savitzky-Golay algorithm in a frequency range between 1800 and 900 cm^{-1}. The spectra were first vector normalized over the investigated frequency range, and then, Ward's algorithm was used to construct dendograms by OPUS 5.5 (Bruker Optic, GmbH). The spectral distance was calculated between pairs of spectra as Pearson's product moment correlation coefficient.[19] Since sensitivity and specificity can be used in the performance of the methods used in diagnosis of a disease state, these parameters were calculated as performed in Severcan et al.[19] Briefly, negative (true and false) and positive values (true and false) were identified according to epileptic and nonepileptic samples. The identification of sensitivity and specificity values

dx.doi.org/10.1021/ac402992j | Anal. Chem. 2014, 86, 1395−1403

Table 1. Frequency and Peak Area Values of FT-IR Bands for Control, Low Dose, and High Dose of PTZ for Rat Brain Homogenate[a]

functional group	control (n = 6)	low dose PTZ (n = 6)	high dose PTZ (n = 6)
	Frequency Values		
C═O	1736.09 ± 0.07	1734.72 ± 1.37[b]	1732.17 ± 1.39[b]
PO^-_2 asymmetric	1236.88 ± 3.45	1225.40 ± 1.15[b]	1223.32 ± 0.87[b]
C−O asymmetric	1171.88 ± 1.02	1171.85 ± 0.29	not observed
CO−O−C asymmetric	1156.95 ± 0.18	1155.80 ± 0.18	not observed
PO^-_2 symmetric	1080.92 ± 0.58	1077.92 ± 2.76[b]	1062.58 ± 2.12[b]
C^+−N−C	998.91 ± 0.12	992.21 ± 0.65[b]	1001.98 ± 0.51[b]
	Band Area Ratio Values		
lipid/protein	0.56 ± 0.002	0.58 ± 0.003	0.59 ± 0.004[b]
CH_2 asymmetric/lipid	0.60 ± 0.001	0.57 ± 0.002[b]	0.52 ± 0.003[b]
C═O/lipid	0.28 ± 0.004	0.27 ± 0.002	0.26 ± 0.001[b]
HC═CH/lipid	0.059 ± 0.0004	0.062 ± 0.0002[b]	0.064 ± 0.0001[b]
glycogen/lipid	0.25 ± 0.003	0.19 ± 0.002	
RNA/protein	0.08 ± 0.003	0.10 ± 0.002[b]	0.17 ± 0.001[c]

[a]The values are the mean ± standard deviation for each sample. [b]Degree of significance: $p < 0.05$*. [c]Degree of significance: $p < 0.01$**.

were shown in Table 2 in the Supporting Information; more information can be obtained from Severcan et al.[19]

Statistical Analysis. The differences in the means of control and treated groups were compared using the analysis of variance (ANOVA) statistical test, and the results were expressed as mean ± standard deviation. A p value of less than 0.05 was considered significant ($p < 0.05$*, $p < 0.01$**).

RESULTS

The current study aimed to investigate the effects of epileptic seizures induced by subconvulsive (25 mg/kg) and convulsive (60 mg/kg) doses of PTZ on rat brain homogenates using FT-IR spectroscopy. FT-IR spectra of control and PTZ groups showed distinctive absorption modes over the wavenumber range of 3050−900 cm^{-1}. They were assigned to specific molecular groups on the basis of published studies[14−18,30−33] in the Supporting Information. To observe the details of the spectral analysis, the spectra were investigated in two regions. Figure 1A,B show normalized infrared spectra of control, subconvulsive, and convulsive doses of PTZ of rat brain homogenates in the 3050−2800 cm^{-1} and 2000−900 cm^{-1} regions, respectively. In Figure 1A, the spectra were normalized with respect to the CH_2 asymmetric stretching band at 2925 cm^{-1}, and in Figure 1B, the spectra were normalized with respect to the amide I band at 1645 cm^{-1} for visual demonstration of the spectral variations. As shown in Figure 1A,B and Table 1, there are remarkable differences in the spectral parameters of the control and PTZ treated groups.

The frequency values of absorptions are shown in Table 1. As illustrated in Table 1 and Figure 1A,B, PTZ-induced seizures led to significant ($p < 0.05$*) shiftings to lower values in the C═O (1736 cm^{-1}), the PO^-_2 asymmetric (1236 cm^{-1}), and the PO^-_2 symmetric (1080 cm^{-1}) but higher values in the C^+−N−C stretching (998 cm^{-1}). On the other hand, the modes from the C−O stretching in glycogen (1173 cm^{-1}) and the CO−O−C asymmetric stretching in cholesteryl esters (1156 cm^{-1}) diminished in the spectrum of convulsive dose of PTZ as depicted in Figure 1B.

Alterations in fluidity of the membrane can be monitored by probing the CH_2 asymmetric stretching mode in the C−H region (3050−2800 cm^{-1}). The bandwidth value of this band provides information about the dynamics of the system.[17,30] Both subconvulsive (12.18 ± 2.13*) and convulsive (12.01 ± 0.83*) doses of PTZ brought about a reduction compared to the control group (13.98 ± 0.67) in the bandwidth values of this mode. This indicates a decrease in the lipid dynamics, which also suggests less fluid membrane structure upon PTZ-induced seizures.[15]

Even though every effort had been made in FT-IR spectroscopic studies to remove the artifacts that might arise from experimental conditions such as sample thickness, the area ratios of some specific infrared bands have been evaluated for relative quantitative comparison between the control and the treated samples. The ratio values for the control, subconvulsive, and convulsive doses of PTZ are displayed in Table 2. Detailed information for the calculation of the ratios was given in the Supporting Information. According to the results, there was a significant ($p < 0.05$*) increase in lipid/protein, RNA/protein, and olefinic HC═CH/lipid ratios for PTZ groups. The increment in olefinic/lipid ratio was confirmed by TBARS assay. MDA levels were found to be 7.98 ± 1.28 nmol/mg protein for the control samples, 11.32 ± 2.09 nmol/mg protein ($p < 0.05$*) for low dose of PTZ, and 14.11 ± 1.07 nmol/mg protein ($p < 0.05$*) for high dose of PTZ (Supporting Information, Figure S-3). Also, the ratio values of CH_2/lipid, C═O/lipid, COO^-/lipid, and glycogen/lipid were found to be significantly ($p < 0.05$*) reduced in PTZ groups compared to the control group.

Table 2. Changes in Value of Protein Secondary Structure Estimation by NN Predictions for Control, Low Dose, and High Dose of PTZ for Rat Brain Homogenate[a]

functional groups	neural network predictions: control (n = 6)	low dose PTZ (25 mg/kg) (n = 6)	high dose PTZ (60 mg/kg) (n = 6)
α helix	17.5 ± 0.5	17.9 ± 0.6	20.2 ± 1.1[b]
β sheet	57.3 ± 2.9	51.5 ± 3.1[b]	49.5 ± 2.3[b]
turns	14.5 ± 2.6	16.6 ± 1.9[b]	16.7 ± 1.4
random coil	10.7 ± 1.3	13.8 ± 0.9[b]	13.9 ± 1.7[b]

[a]The values are the mean ± standard deviation for each sample. [b]Degree of significance: $p < 0.05$*.

In order to examine the changes in protein secondary structure, the amide I band between 1700 and 1600 cm^{-1} was

dx.doi.org/10.1021/ac402992j | Anal. Chem. 2014, 86, 1395−1403

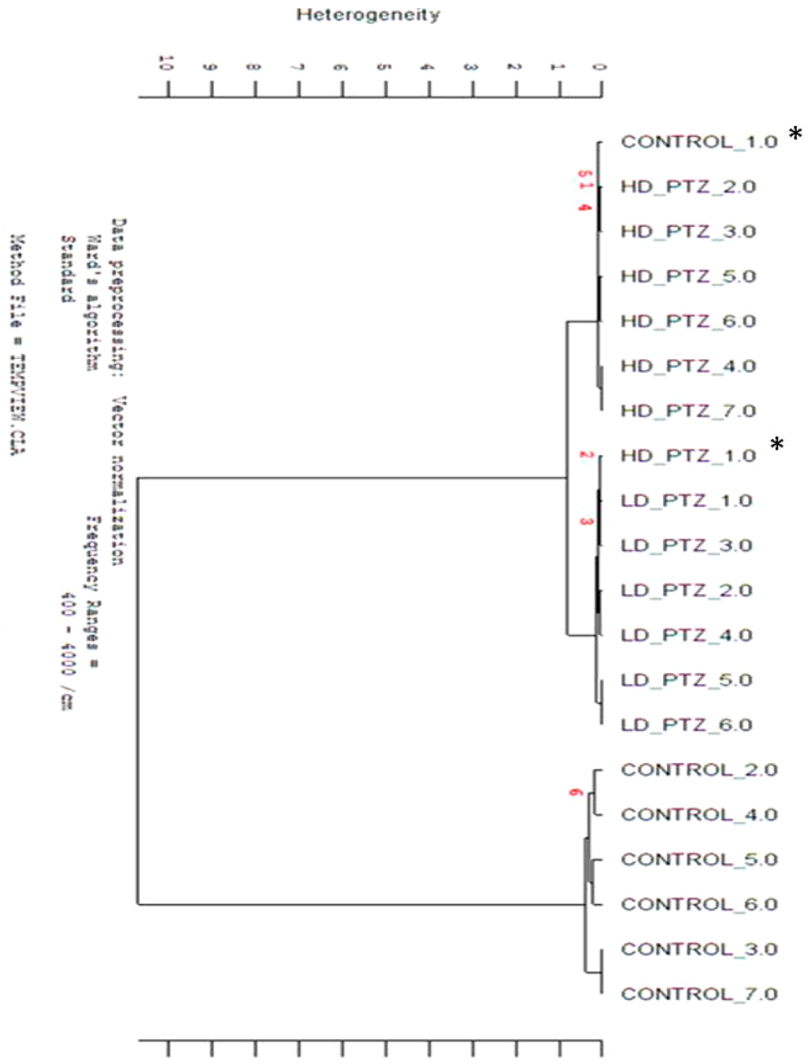

Figure 2. Hierarchial clustering of control, low dose, and high dose of PTZ in the 1800−900 cm^{-1} spectral range. The sample labeled with * was not clearly differentiated and not evaluated in the statistical analysis.

analyzed using NNs as previously applied to protein in solutions[28] and in tissues.[14,15,17,33] As demonstrated in Table 2, both low and high doses of PTZ induced a significant decrease ($p < 0.05$*) in β sheet and a significant increase in α helix and random coil structure.

On the basis of these spectral differences, cluster analysis was applied to the control and PTZ injected groups and the resultant dendrogram is presented in Figure 2. As depicted in the figure, three distinct clusters were produced with a high accuracy with success of (6/7) for control, (6/6) for low dose, and (6/7) for high dose PTZ-treated samples, respectively. Table 3 in the Supporting Information represents the sensitivity and specifity parameters for treated groups. The sensitivity and specificity is 100% for the low dose PTZ group. However, for the high dose PTZ group, 85% specifity and 85% sensitivity were found.

■ DISCUSSION

Taking advantage of FT-IR spectroscopy, the current study was conducted to determine the effects of two different doses of PTZ on rat brain homogenate by monitoring the variations in the frequencies, bandwidths, and peak areas of the vibrational modes of macromolecules. Unsaturated lipids readily react with free radicals and undergo peroxidation. When lipid peroxidation occurs, a decrease in the intensity/area of olefinic mode and subsequently in the olefinic =CH/lipid ratio is expected as reported by Leskovjan et al.[34] and others.[14,18] However, alternatively, if there is an increment in lipid peroxidation end products, which contain a =CH group, an increase in the olefinic band (3012 cm^{-1}) area can be observed. In our study, the rise in the olefinic band area due to PTZ treatment indicates an increase in lipid peroxidaton end products as also supported by TBAR assay (Supporting Information, Figure S-4). The reason of such outcome might be that the loss of unsaturation was compensated by the presence of =CH groups in lipid peroxidation end-products such as lipid aldehydes and alkyl radicals, as obtained in our studies[14,15,17,18,35] and other reports.[36−38] On the other hand, it was also reported that the presence of lipid peroxidation end products such as MDA may contribute to an increased peak area of the C═O mode (1736 cm^{-1}).[17] However, in the present study, we recorded a decrease in the ratio of C═O/lipid in PTZ-treated groups. The C═O mode arises from triglycerides, cholesterol esters, and phospholipids.[17,35,39] All these biomolecules are highly utilized in demand for high neuronal activity during epileptic seizures as further supported by lowered CH_2/lipid and COO^-/lipid

dx.doi.org/10.1021/ac402992j | Anal. Chem. 2014, 86, 1395−1403

ratios. Since there was a high degree of degradation of these molecules, the presence of C═O groups, especially from MDA, might not have compensated for such decrease. Our finding is in accordance with earlier studies that investigated different parts of the brain,[40] as well as other models of epileptic seizures.[41]

The presence of lipid peroxidation end products upon seizure induction by PTZ application might be the outcome of some processes such as dysfunction of the mitochondrial respiratory chain (MRC) and the production of arachidonic acid (AA) during a high rate of neuronal activity. MRC is the major source of reactive oxygen species (ROS) and nitric oxide (NO) in cells. The attack of ROS on lipids in the mitochondrial membrane together with the interaction of NO with cyctochrome c oxidase and complexes II and III leads to defected oxidative phosphorylation. The inhibition of oxidative phosphorylation coupled with the increased utilization of energy during epileptic activity interrupts the cell's capability to maintain energy levels, subsequently causing mitochondrial damage. Mitochondrial dysfunction, defected oxidative phosphorylation, and reduced energy levels during seizures have been reported previously.[42] Nevertheless, MRC dysfunction along with elevated free radicals could also trigger the apoptotic pathways in the epileptic condition.[43]

There is another possible explanation for the source of lipid peroxidation end products during epileptic convulsions. Throughout high neuronal activity, the release of glutamate takes place and glutamate neuronal receptors are initiated which in turn activates phospholipases to produce AA.[44] Afterward, AA is metabolized to produce ROS, covalently bind to cellular proteins, and alter their function.[45] Hence, the over production of ROS is related to contributing to membrane malfunction, excitotoxicity, neuronal injury, and cell death in both long-term[16] and short-term seizure activity.[46]

Abnormal lipid metabolism is also involved in the pathogenesis of epilepsy.[47] Any change in lipid structure may account for cytological changes in cellular properties like variability in size/shape and alteration in the extracellular matrix observed in epileptic conditions. The alterations in the content and structure of lipids after PTZ-induced seizures were observed as variations in the spectral changes in the bands attributed to unsaturated lipids, cholesterol esters, cholesteryl esters, phospholipids, and fatty acids.[14,17,20,35] A decline in the ratios of C═O/lipid, CH_2/lipid, and COO^-/lipid might indicate a decreased amount of triglycerides, cholesterol esters, and saturated lipids and fatty acids, respectively, which might be due to breakdown of these molecules during epileptic activity. The presence of these perturbations in lipid content could be a precondition for the development and expression of this disorder. A similar finding was also reported that the administration of U18664, which is the initiator of chronic seizures, decreased the concentration of brain phospholipids through inhibition of phospholipid synthesis.[48]

The shifting of frequencies of the C═O (1736 cm^{-1}), the PO^-_2 asymmetric (1236 cm^{-1}), and the PO^-_2 symmetric (1080 cm^{-1}) modes to lower values, more profound for a convulsive dose of PTZ, means that PTZ-induced epileptic activity increased the hydration state of the glycerol backbone near the hydrophilic part and polar headgroup of the membrane lipids, respectively.[23,24] This may introduce a difference in the packing of phospholipid molecules.[31] This has been reported to originate from the reaction between free radicals and membrane proteins or lipids, which may increase a cross-linking between these membrane components.[49] Altered composition of membrane phospholipids results in changes in the activity and kinetic parameters of membrane proteins, such as synaptic Mg^{2+}- and Ca^{2+}-dependent ecto-ATPase which primarily have an important role in neuronal activity. The decrease in the activity of Ca^{2+} and Mg^{2+} pumps causes a further decrease in neuronal energy which is suspected to play a particular role in seizure-related neuronal damage.[50]

The disruption of membrane organization is directly associated with the decrease in membrane fluidity observed by a decrease in the bandwidth values of the CH_2 asymmetric (2923 cm^{-1}) and the CH_2 symmetric (2852 cm^{-1}) bands. Decreased membrane fluidity leads to activity changes or inhibition of membrane-bound enzymes, ion channels, and receptors.[51,52] The difference in membrane fluidity together with the changes in the packing of membrane phospholipids may encounter the dysfunction of glucose transporters in the blood brain barrier (BBB). As a result, cerebral blood flow does not compensate the metabolic demand. Thus, apparent net energy impairment occurs in the brain. This energy failure can give rise to the loss of ionic homeostasis considered to be one of the important effects generating epileptic activity. Taking into consideration that especially potassium ion homeostasis plays a crucial role in initiating the epileptic activity, it is likely that the Na/K ATP-ase mechanism, other than voltage-dependent potassium uptake, provides efficient potassium buffering, which produces an increase in metabolic demand due to the ATP requirement of the pump.[51,52] All mentioned events trigger the uncoupling of metabolic demand and expenditure, which may accelerate a variety of mechanisms underlying epileptic activity such as decreased inhibition of neuronal depolarization.

Increased lipid/protein ratio suggests that there was a more pronounced decrease in protein content when compared with those of lipid content. This decrease might be from protein degradation and disruption. Damage to proteins can result from the attack of free radicals, which may lead to increased susceptibility to proteolysis, tissue damage, and neurotoxicity. The decrease in protein content may also result from down regulation of some specific proteins such as dopamine D1 and D2 receptors[53] and siRNA mediated GABAB1 receptor[54] which have been reported upon PTZ-induced seizures in the literature. According to our results, the convulsive dose of PTZ was more effective to decrease protein content compared to the subconvulsive dose. On the contrary, the variations in the lipid to protein ratio have a very important effect on membrane structure and dynamics.[52] These changes may be reflective of the alterations of lipid and protein asymmetry which directly affect membrane structure and fluidity and consequently may cause alterations in the membrane potential via ion channel kinetics.[14,24] This may play a fundamental role in the generation of epileptic seizures, as well. Thus, this observed alteration could be accepted as an early consequence of PTZ-induced epileptic activity using FT-IR spectroscopy.

We first investigated epileptic convulsion-induced changes in protein conformation without the need for the application of isolation procedures by NNs method as previously applied to determine protein secondary structure in tissues and membranes.[14−17] Since FT-IR spectroscopy cannot distinguish specific proteins, all data obtained from NNs analysis have provided information about all proteins including extracellular, plasma membrane, cytoplasm, and nuclear proteins. The results of NNs predictions are presented in Table 2. It is clearly

evident from the table that both low and high doses of PTZ administration caused a significant decrease in β sheet and an increase in random coil structures. From this result, it can be deduced that PTZ-stimulated epileptic seizures led to altered protein secondary structure in the system.[17,55] As reported in the literature, a variety of proteins like neurotransmitter receptors and ion channels undergo structural and functional alterations in epileptic loci in the brain.[56−58] One possible explanation for this variation may be the attack of free radicals to proteins, which is a phenomenon observed in epileptic activities.[14,58] These radicals are reported to cause differences in proteins' primary, secondary, and tertiary structure, and therefore, proteins may undergo spontaneous fragmentation during high neuronal activity.[58] Another explanation may be a high degree of intracellular acidosis. According to the literature,[59] high neuronal activity promotes accumulation of lactate, which results in low intracellular pH of neurons. Lowering pH can give rise to some changes in the protein structure.[60] Moreover, the altered redox potential resulting from the changes in Ca^{2+} and K^{+} currents as seen during epileptic seizures could profoundly modify the structure of proteins.[60] In addition, involvement of heat shock proteins in the process of epilepsies has been previously reported.[61,62] Deterioration of these proteins may be responsible for misfolding. For example, an important member of this family, Hsp60, involves improper folding of mitochondrial proteins. The dysfunction of Hsp60 has been shown to bring out increased misfolded proteins in epileptic hippocampus.[62] Additionally, some variations in membrane lipids content and their structures, as also observed by a decrease in C═O/lipid, COO^{-}/lipid, and CH_2/lipid ratios and shiftings in the C═O and the PO^{-}_2 modes in the current study, leads to altered membrane thickness.[35] This alteration triggers structural differences in membrane proteins toward an increase in unordered proteins which include protein denaturation.[35,63] In this regard, all mentioned explanations might be responsible for the different protein profiles in the brain after PTZ-induced seizures. NNs results are reflective of defects in protein functioning which can possibly provoke seizures and pathogenesis of epileptic condition. Indeed, structural changes in proteins may probably alter the phospholipid behavior in membranes such as membrane dynamics.[64] Overall, reported findings may also have significance regarding the regulation of membrane functions of the brain in epileptogenesis. Furthermore, it is worth mentioning that these kinds of changes in protein structure are observed not only in epileptic condition but also in several diseases.[65−68]

We have also found that two different doses of PTZ administration both caused a reduction in glycogen content obtained by lowered ratio of glycogen/lipid. This result might be directly related to energy demands during epileptic activity. Stimulated neuronal activity as seen in PTZ-induced seizures requires energy produced by nonoxidative glycolysis which leads to an accumulation of lactate. Stimulated neuronal epileptic activity creates an uncoupling of glucose consumption and oxidation mainly caused by the altered activity of glucose transporters in the structure of BBB.[69] Such uncoupling appears to be compensated by glycogen. The increase in nonoxidative glycolysis is a normal metabolic process used to support glutamate/GABA metabolism during enhanced neuronal activity. The majority of glucose required to fuel the pumping of glutamate from the synaptic cleft during intense bursts of activity is provided by the glycogen in the brain. There is *in vivo* evidence that brain glycogen may be rapidly mobilized to support the physiologic brain activation.[70] Taking this into consideration, the disappearance of the glycogen band located at 1170 cm^{-1} in the convulsive group can be explained by the high rate of utilization of glycogen during epileptic activity. Thus, these metabolic changes induced by PTZ suggest that seizures might be indicative of cell stress in rat brains.

Upon PTZ administration, the shifting of the frequencies of nucleic acid bands (1236, 1080, and 998 cm^{-1}) might also be due to the structural alterations of nucleic acids, susceptible to seizure-induced oxidative stress. Indeed, in this study, the ratio of RNA/protein significantly increased for PTZ convulsive dose in comparison to the control and subconvulsive groups indicating high RNA content. This further suggests an increase in RNA production reflecting the high degree of protein synthesis. These findings are in accordance with the results of a previous study in which gene transcriptions for three immediate early genes, c-fos, c-jun, and NGFI-A, and three neuropeptide genes, enkephalin, dynorphin, and neuropeptide Y, increased following a single injection of convulsant PTZ. Among these genes, especially c-fos has been reported to be induced in neurons following the increase in intracellular calcium levels. Therefore, this gene is responsible for molecular events leading to the permanent changes in brain underlying epilepsy and neural plasticity in kindling.[71] Hence, these results reveal dose-dependent effects of PTZ-induced seizures on the level of gene expression, which can also be detected by FT-IR spectroscopy.

Finally, cluster analysis based on the FT-IR spectra in the 1800−900 cm^{-1} region provided successful differentiation with a high accuracy (success rate: 6/7 for control, 6/6 for low dose, and 6/7 for high dose) (Supporting Information, Figure S-3). The 100% value of specifity and sensitivity for the low dose PTZ group reveals a high degree of differentiation. On the other hand, the lower specifity value of the high dose PTZ group might be reflected as the appearance of a high dose PTZ spectrum within the low dose cluster, also meaning a low degree of heterogenity. In this case, the spectrum that was merged into a different cluster was not involved in statistical calculations. Hence, epileptic activities stimulated by low and high doses of PTZ administration give rise to important changes in FT-IR spectra which can be effectively determined by the application of cluster analysis.

■ CONCLUSION

In order to foster efficient diagnosis and a treatment strategy for epilepsy, basic research is essential to clarify mechanisms lying under epileptogenesis depending on both its causes and consequences, eventually on a biochemical and molecular basis. An understanding of these facts will facilitate the identification of epilepsy biomarkers and the development of specific drug therapies to target the particular defects causing generation of epileptic conditions.

The current study demonstrates distinctive spectral parameters resulting from molecular actions under PTZ-induced convulsions for the first time. An increase in lipid peroxidation end products, RNA amount, and structural differences in proteins, lipids, and nucleic acids were identified. Furthermore, a decline in protein, lipid, and glycogen content was detected. It was also found that PTZ-induced seizures led to a decrease in membrane fluidity and differences in packing of membrane components. NNs analysis provided significant insights into the changes in protein secondary structure, here exemplified by a decrease in β sheet and an increase in random coil.

dx.doi.org/10.1021/ac402992j | Anal. Chem. 2014, 86, 1395−1403

Furthermore, cluster analysis based on spectral changes resulted in an excellent grouping of the control and PTZ treated groups. This clearly shows the use of FT-IR spectroscopy for monitoring of epileptic conditions which was previously performed for other diseases.[19,65,68,72−74]

With the aim of shedding light on the mechanisms underlying epilepsy, we determined structural, compositional, and dynamical changes, all of which have the potential to trigger epileptic conditions. The findings of the current study can provide a basis for the research on diagnosis and the development of newly designed antiepileptic agents.

■ ASSOCIATED CONTENT

Supporting Information

Additional information as noted in text. This material is available free of charge via the Internet at http://pubs.acs.org.

■ AUTHOR INFORMATION

Corresponding Author

*Phone: +90-312-210-51-66. Fax: +90-312-210-79-76. E-mail: feride@metu.edu.tr.

Notes

The authors declare no competing financial interest.

■ ACKNOWLEDGMENTS

This study was supported by State Planning Organization of Turkey (DPT/BAP-01-08DPT2003K120920/790) and Scientific and Technical Research Council of Turkey (TUBITAK: SBAG-2940 (104S475)).

■ REFERENCES

(1) De Sousa, D. P.; Gocalves, J. C. R.; Quintans, L. *Neurosci. Lett.* **2006**, *401*, 231−235.
(2) Commission on Epidemiology and Prognosis of the International League Agaist Epilepsy (ILAE). *Epilepsia* **1993**, *34*, 592−596.
(3) Cockerell, O.; Johnson, A. L.; Shorvon, S. D. *Prognosis Epilepsy* **1997**, *38*, 31−46.
(4) De Lorenzo, R. J.; Sun, D. A.; Deshpande, L. S. *Pharmacol. Ther.* **2005**, *105*, 229−266.
(5) Yildirim, M.; Marangoz, C. *Brain Res.* **2006**, *1099*, 183−188.
(6) Uribe-Escamilla, R.; Mota-Rojas, D.; Sanchez-Aparicio, P. *Seizure* **2007**, *16*, 397−401.
(7) Bloms-Funke, P.; Madeja, M.; MuBhoff, U.; Speckmann, E. J. *Neurosci. Lett.* **1996**, *205*, 115−118.
(8) Madeja, M.; MuBhoff, U.; Lorra, C.; Pongs, O.; Speckmann, E. J. *Brain Res.* **1996**, *722*, 59−70.
(9) Turker, S.; Wassall, S.; Stillwell, W.; Severcan, F. *J. Pharm. Biomed. Anal.* **2011**, *54*, 5−10.
(10) Erakovic, V.; Zupan, G.; Varlijen, J. *Neurochem. Int.* **2003**, *42*, 173−178.
(11) Eloqayli, H.; Dahl, C. B.; Gotesman, K. G.; Unsgard, G. *J. Neurochem.* **2003**, *85*, 1200−107.
(12) Pitkanen, A.; Nissinen, J.; Jolkkonen, E.; Tuunanen, J.; Halonen, T. *Epilepsy Res.* **1999**, *33*, 67−85.
(13) Patel, M.; Liang, L.; Roberts, L. *J. Neurochem.* **2001**, *79*, 1065−1069.
(14) Cakmak, G.; Zorlu, F.; Severcan, M.; Severcan, F. *Anal. Chem.* **2011**, *83*, 2438−2444.
(15) Bozkurt, O.; Severcan, M.; Severcan, F. *Analyst* **2010**, *135*, 3110−3119.
(16) Aksoy, C.; Guliyev, A.; Kılıc, E.; Uckan, D.; Severcan, F. *Stem Cells Dev.* **2012**, *15*, 45−49.
(17) Ozek, N. S.; Tuna, S.; Erson-Bensan, A. E. *Analyst* **2010**, *135*, 3094−3102.
(18) Severcan, F.; Gorgulu, G.; Gorgulu, S. T.; Guray, T. *Anal. Biochem.* **2005**, *339*, 36−40.
(19) Severcan, F.; Bozkurt, O.; Gurbanov, R.; Gorgulu, G. *J. Biophotonics* **2010**, *3*, 621−631.
(20) Petibois, C.; Deleris, G. *Trends Biotechnol.* **2006**, *24*, 455−462.
(21) Galli, R.; Uckermann, O.; Winterhalder, M.; Sitoci-Ficici, K.; Kirsch, M. *Anal. Chem.* **2012**, *84*, 8707−8714.
(22) Petit, V.; Refregiers, M.; Guettier, C. *Anal. Chem.* **2010**, *82*, 3963−3968.
(23) Toyran, N.; Zorlu, F.; Severcan, F. *Int. J. Radiat. Biol.* **2005**, *81* (12), 911−918.
(24) Akkas, S. B.; Severcan, M.; Yilmaz, O. *Food Chem.* **2007**, *105*, 1281−1288.
(25) Racine, R. J. *Electroencephalogr. Clin. Neurophysiol.* **1972**, *32*, 281−289.
(26) Sivakumar, S.; Sivasubramaniana, J.; Raja, B. *Mol. Biomol. Spect.* **2012**, *99*, 252−258.
(27) Chouhan, S.; Flora, S. J. S. *Toxicology* **2008**, *254*, 61−67.
(28) Haris, P. I.; Severcan, F. *J. Mol. Catal. B: Enzym.* **1999**, *7*, 207−221.
(29) Severcan, M.; Severcan, F.; Haris, I. P. *Anal. Biochem.* **2004**, *332*, 238−244.
(30) Melin, A.; Perromat, A.; Deleris, G. *Biopolymers (Biospectroscopy)* **2000**, *57*, 160−168.
(31) Chiriboga, L.; Yee, H.; Diem, M. *Appl. Spectrosc.* **2000**, *54*, 480−485.
(32) Banyay, M.; Sarkar, M.; Gräslund, A. *Biophys. Chem.* **2003**, *104*, 477−488.
(33) Garip, S.; Yapici, E.; Ozek, N.; Severcan, M.; Severcan, F. *Analyst* **2010**, *135*, 3233−3241.
(34) Leskovjan, A. C.; Kretlow, A.; Miller, L. M. *Anal. Chem.* **2010**, *82*, 2711−2716.
(35) Ozek, N.; Bal, B.; Sara, Y.; Onur, R.; Severcan, F. *Biochim. Biophys. Acta, Gen. Subj.* **2014**, *1840*, 406−415.
(36) Yin, H.; Xu, L.; Porter, N. A. *Chem. Rev.* **2011**, *111*, 5944−5972.
(37) Liu, K. Z.; Bose, R.; Mantsch, H. H. *Vib. Spectrosc.* **2002**, *28* (1), 131−136.
(38) Liu, K. Z.; Shi, M. H.; Mantsch, H. H. *Blood Cells, Mol., Dis.* **2005**, *35*, 404−412.
(39) Cakmak, G.; Miller, L.; Zorlu, F.; Severcan, F. *Arch. Biochem. Biophys.* **2012**, *520*, 67−73.
(40) Patsoukis, N.; Zervoudakis, G.; Georgiou, C. D. *Epilepsia* **2005**, *46*, 1205−1211.
(41) Bellissimo, M. I.; Amado, D.; Abdalla, D. S. P.; Ferreira, E. C.; Cavalheiro, E. A. *Epilepsy Res.* **2001**, *46*, 121−128.
(42) Archaya, M. M.; Katyare, S. S. *Exp. Neurol.* **2005**, *192*, 79−88.
(43) Cock, H. R. *Prog. Brain Res.* **2002**, *135*, 187−196.
(44) Adibhatla, R. M.; Hatcher, J. F.; Dempsey, R. J. *AAPS Natl. Biotechnol. Conf. Symp. Lipidomics* **2006**, *8*, 36.
(45) Nigam, S.; Schewe, T. *Biochim. Biophys. Acta* **2000**, *1488*, 167−181.
(46) Akbas, S. H.; Yegin, A.; Ozben, T. *Clin. Biochem.* **2005**, *38*, 1009−1014.
(47) Ma, X.; Liu, G.; Wang, S.; Chen, Z.; Lai, M.; Liu, Z.; Yang, J. *J. Chromatogr., B* **2007**, *859*, 170−177.
(48) Cenedella, R. J.; Sarkar, C. P. *Biochem. Pharmacol.* **1984**, *33*, 591−598.
(49) Phillis, J. W.; Horrocks, L. A.; Farooqui, A. A. *Brain Res.* **2006**, *52*, 201−243.
(50) Walton, N. Y.; Nagy, A. K.; Treiman, D. M. *J. Mol. Neurosci.* **1999**, *11*, 233−242.
(51) Ray, P.; Ray, R.; Broomfield, C. A.; Berman, J. D. *Neurochem. Res.* **1994**, *19*, 57−63.
(52) Bruehl, C.; Hagemann, G.; Witte, O. W. *Epilepsia* **1998**, *39*, 1235−1242.
(53) Tchekalarova, J.; Sotiriu, E.; Georgiev, V.; Angelatou, F. *Brain Res.* **2005**, *1032*, 94−103.
(54) Naseer, M. I.; Lee, H.; Ullah, N.; Ullah, I.; Park, M.; Kim, M. *Synapse* **2010**, *64*, 181−190.

(55) Ozek, N.; Sara, Y.; Onur, R.; Severcan, F. *Biosci. Rep.* **2010**, *30*, 41−50.
(56) Coulter, D. A. *Int. Rev. Neurobiol.* **2001**, *45*, 237−252.
(57) Biervert, C.; Schroeder, B. C.; Kubisch, C. *Science* **1998**, *279*, 403−406.
(58) Waldbaum, S.; Patel, M. *Epilepsy Res.* **2010**, *88*, 23−45.
(59) Chesler, M.; Kaila, K. *Trends Neurosci.* **1992**, *15*, 396−402.
(60) Siesjo, B. K. *Neurochem. Pathol.* **1988**, *9*, 31−88.
(61) Yenari, M. A. *Adv. Exp. Med. Biol.* **2008**, *513*, 281−299.
(62) Liu, X. Y.; Yang, J. L.; Chen, L. J. *Proteomics* **2008**, *8*, 582−603.
(63) Kleinfeld, A. M. *Curr. Top. Membr. Transp.* **1987**, *29*, 1−27.
(64) Szalontai, B.; Nishiyama, Y.; Gombos, Z.; Murata, N. *Biochim. Biophys. Acta* **2000**, *1509*, 409−419.
(65) Turker, S. *Biomed. Spectrosc. Imaging* **2012**, *1*, 303−323.
(66) Ibrahim, M. Z.; Nasse, M. J.; Rak, M.; Hirschmugl, C.; Gough, K. M. *Neuroimage* **2012**, *60*, 376−383.
(67) Szcerbowska-Boruchowska, M.; Dumas, P.; Kastyak, M. Z. *Arch. Biochem. Biophys.* **2007**, *459*, 241−248.
(68) Severcan, F.; Harris, P. *Vibrational Spectroscopy in Diagnosis and Screening*, First ed.; IOS Press: Amsterdam, 2012.
(69) Petroff, O. A. C.; Pan, J. W.; Rothman, D. L. *Epilepsia* **2002**, *43*, 40−50.
(70) Rothman, D. L.; Sibson, N. R.; Hyder, F. *Trans. R. Soc. London (Biol. Sci.)* **1999**, *354*, 1165−1177.
(71) Yount, G. L.; Ponsalle, P.; White, J. D. *Mol. Brain Res.* **1994**, *21*, 219−224.
(72) Toyran, N.; Lasch, P.; Naumann, D.; Turan, B.; Severcan, F. *Biochem. J.* **2006**, *397*, 427−436.
(73) Miller, L. Characterization of neurodegenerative protein misfolding diseases using FTIR spectroscopy and microspectroscopy. In *Vibrational Spectroscopy in Diagnosis and Screening*, First ed.; IOS Press, Amsterdam, 2012; p 118.
(74) Leskovjan, A. L.; Kretlow, A.; Lanzirotti, A.; Barrea, R.; Vogt, S.; Miller, L. M. *Neuroimage* **2011**, *55*, 32−38.